

Supplementary Information

Surface-nitridized 3D nickel host for lithium metal anodes with long cycling life at high-rate

Pan Li^a, Ling Xu^a, Fei Xiong^a, Zihang Zheng^a, Xujian Bao^a, Qiang Ren^a, Yifan Liu^a, Yue Hu^{*b} and Yanwen Ma^{*a}

^a State Key Laboratory for Organic Electronics & Information Displays (SKLOEID), Institute of Advanced Materials (IAM), Nanjing University of Posts & Telecommunications, 9 Wenyuan Road, Nanjing 210023, P.R. China.

^b Key Laboratory of Carbon Materials of Zhejiang Province, College of Chemistry and Materials Engineering, Wenzhou University, Wenzhou 325000, P. R. China.

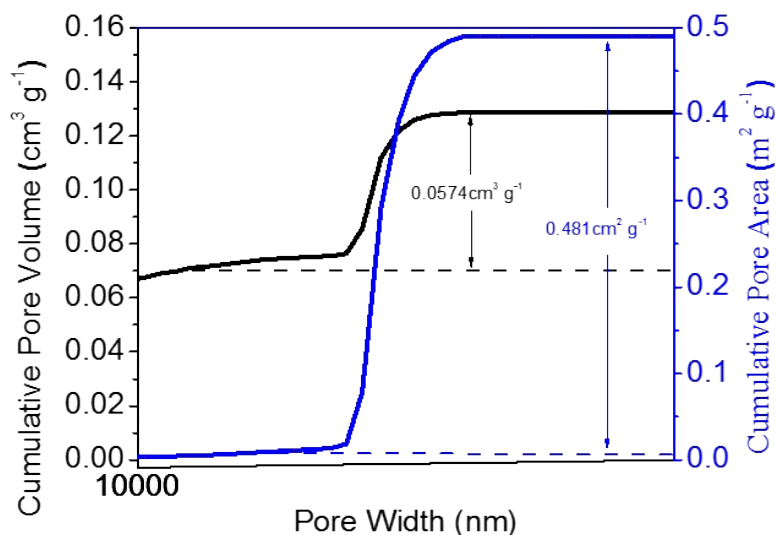


Fig. S1 Porosity analysis for 3D N-Ni structure by mercury porosimetry.

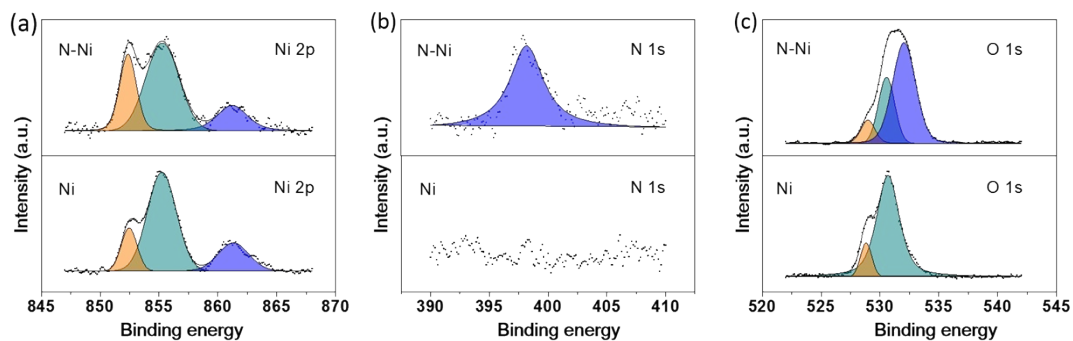


Fig. S2 Surface chemical state analyses of pristine Ni MPs and surface nitridized Ni MPs via XPS. (a) Ni 2p, (b) N 1s, and (c) O 1s spectra of Ni MPs (denoted as Ni) and surface nitridized Ni MPs (denoted as N-Ni) were compared. The binding energy (BE) at 852.7 eV for Ni_3N , was close to that for metallic Ni, which indicated the substantial Ni-Ni bonding.¹ Moreover, the co-presence of Ni_3N and NiO on the surface nitridized Ni MPs was confirmed by the Ni-O peak at 529.7 eV and N 1s peak at 398.2 eV. The peak at 532.64 eV revealed the presence of surface adsorbed oxygen, indicating a significant adsorption activity of the nitridized surface.²

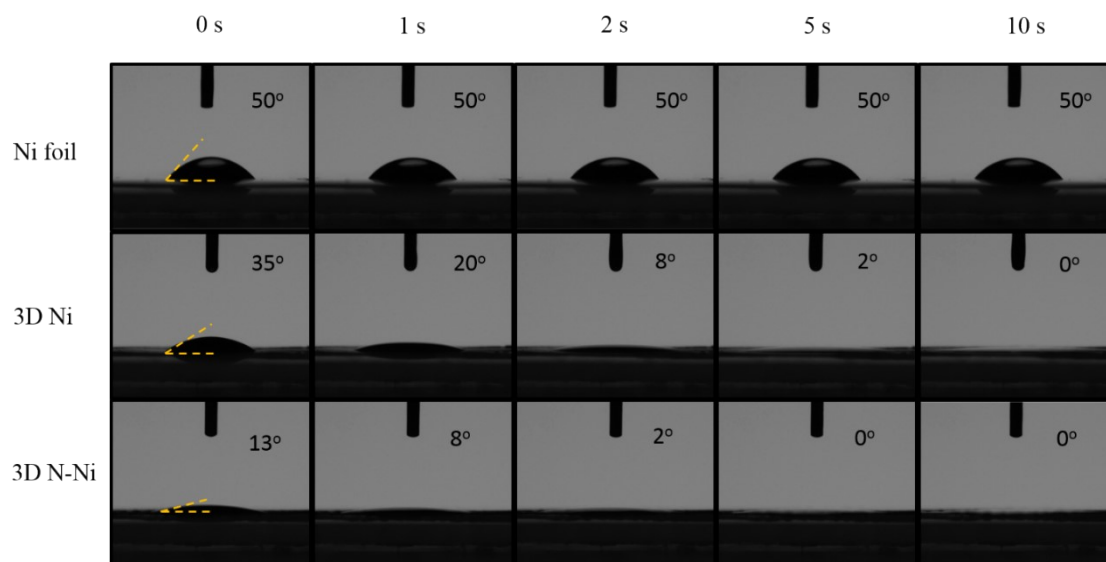


Fig. S3 Dynamic contact angle measurement by the drop shape analyzer during the wetting and diffusion process of the electrolyte on different matrixes.

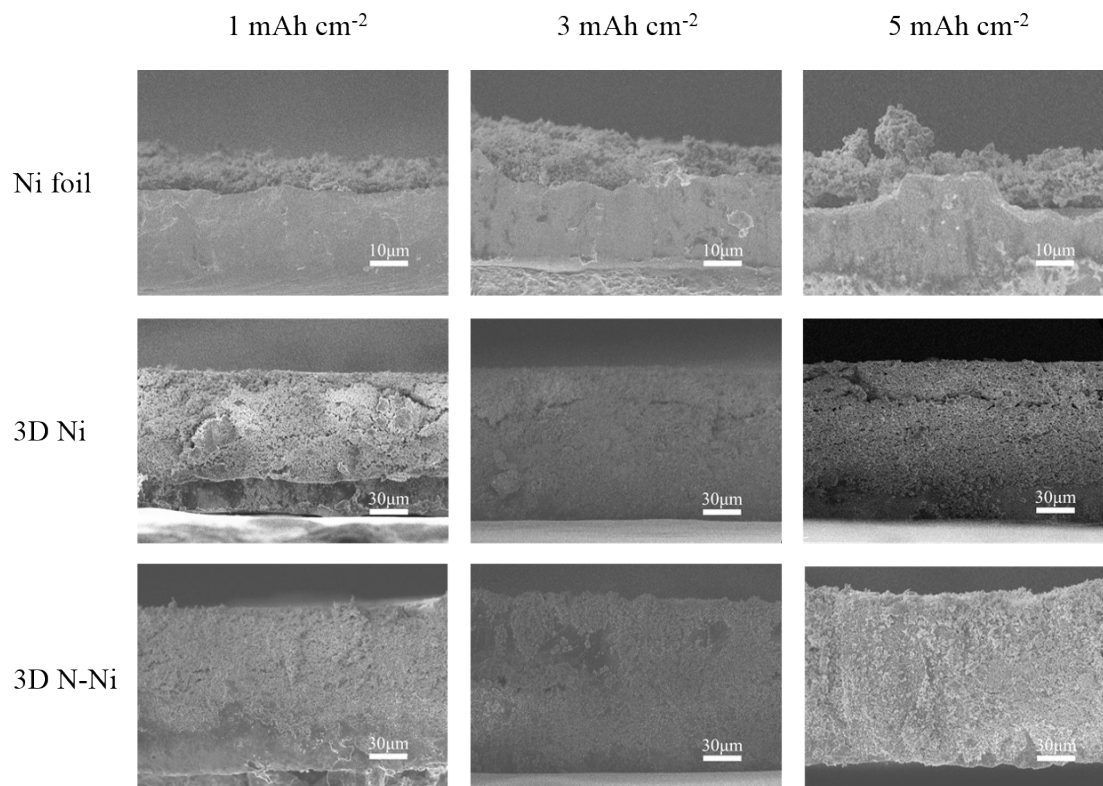


Fig. S4 SEM images of surface morphologies on the side of Ni, 3D Ni and 3D N-Ni matrixes after Li plating with capacities of 1, 3 and 5 mAh cm⁻² under a current density of 1 mA cm⁻².

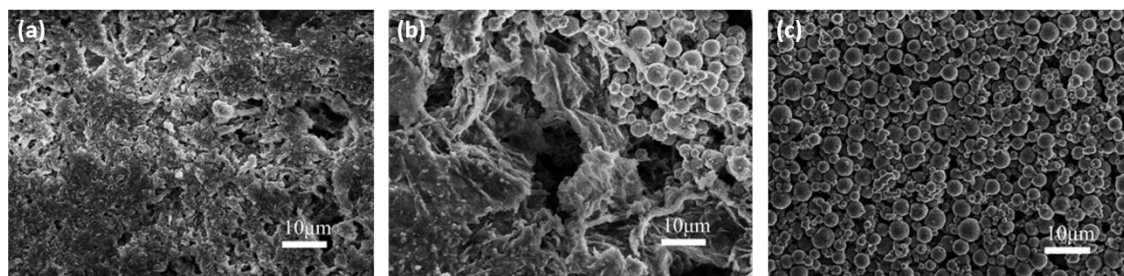


Fig. S5 SEM images of surface morphologies on the top of Ni (a), 3D Ni (b) and 3D N-Ni (c) matrixes after Li stripping at the 50th cycle with capacities of 1mAh cm⁻² under a current density of 1 mA cm⁻².

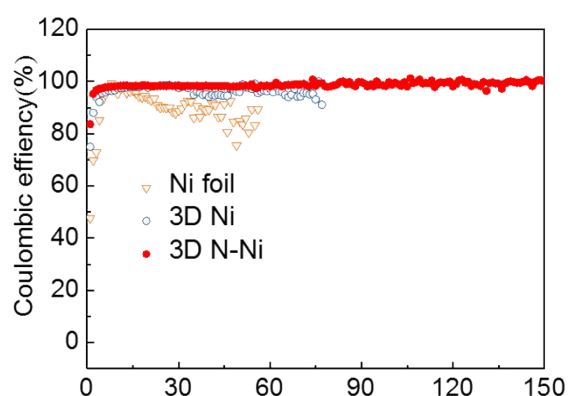


Fig. S6 CE of Li plating/stripping on planar Ni, 3D Ni and 3D N-Ni hosts with current density of 1 mA cm⁻² for a Li capacity of 3 mAh cm⁻².

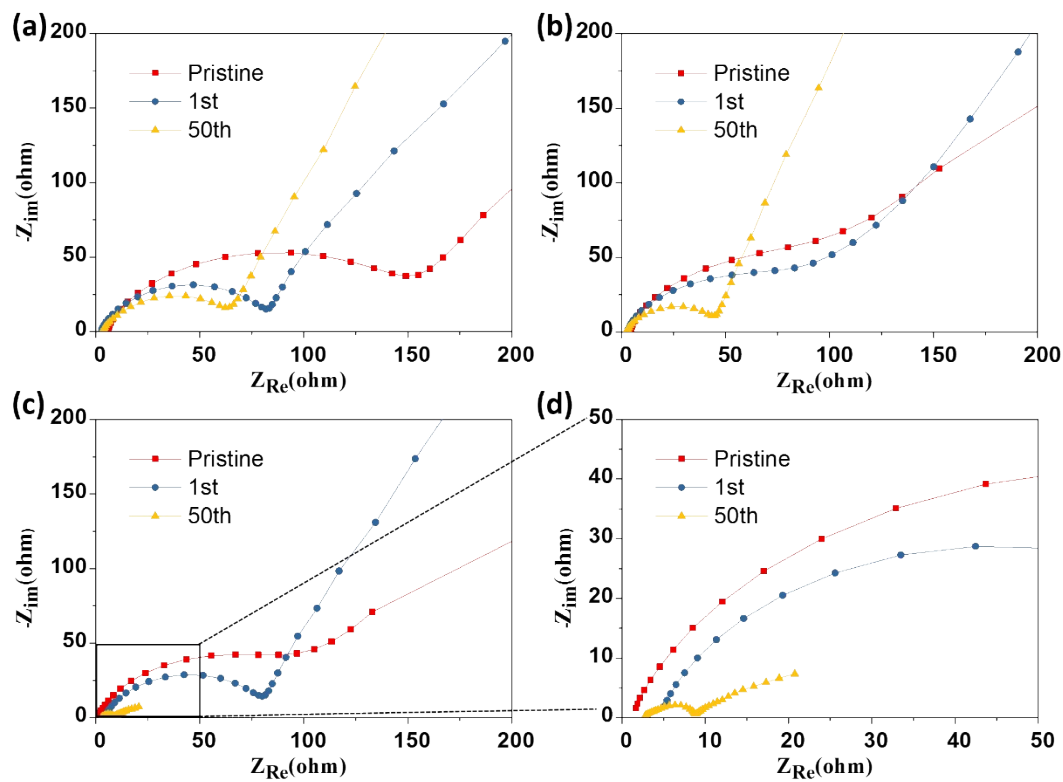


Fig. S7 EIS curves of Ni foil (a), 3D Ni (b) and 3D N-Ni (c, d) electrodes after different cycles (1.0 mA cm⁻², 1.0 mAh cm⁻² of Li).

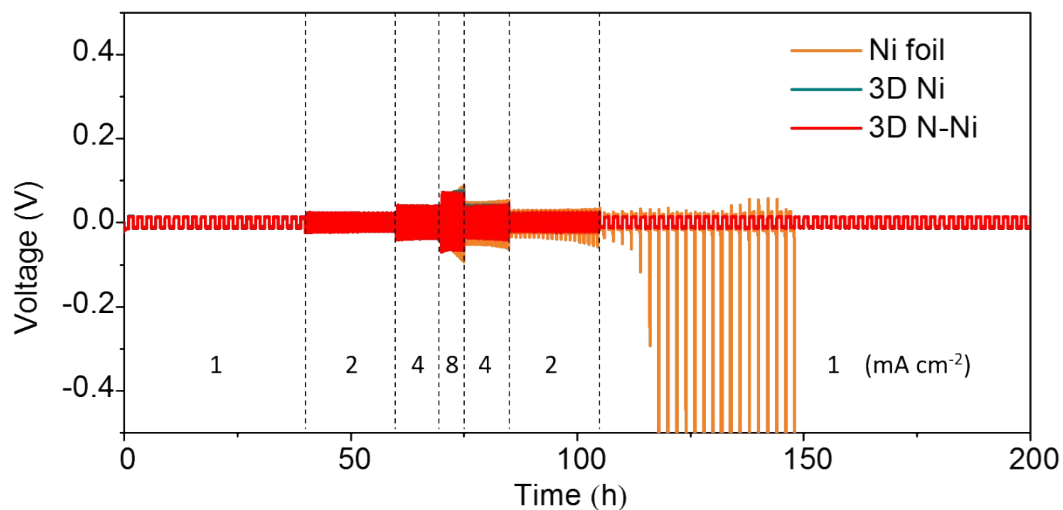


Fig. S8 Voltage profiles of Li plating/stripping with a capacity of 1.0 mAh cm^{-2} on Ni foil, 3D Ni and 3D N-Ni hosts at current densities of 1.0, 2.0, 4.0, 8.0, 4.0 and 2.0 mA cm^{-2} for 20 cycles, and back to 1.0 mA cm^{-2} .

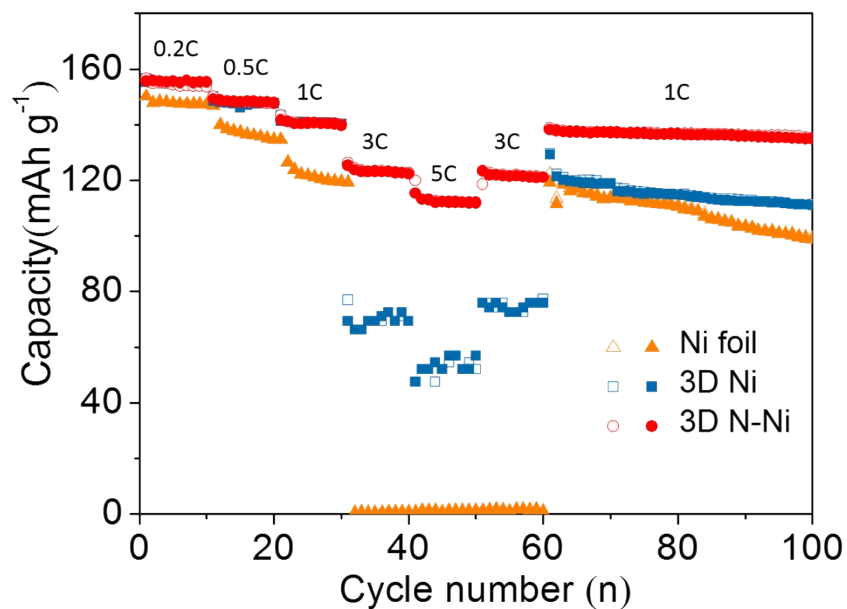


Fig. S9 The rate performance of Li@Ni foil||LFP, Li@3D Ni||LFP and Li@3D N-Ni||LFP cells. All the cells cycled sequentially at 0.2 C, 0.5 C, 1.0 C, 3.0 C, 5.0 C and 3.0 C for 10 cycles at each rate, and back to 1 C, with a total cycle number of 100.

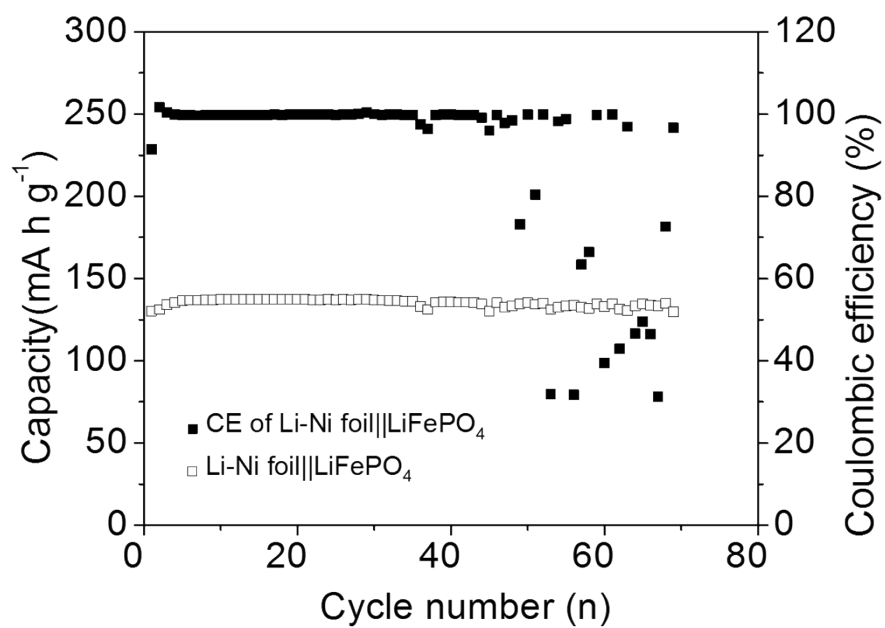


Fig. S10 The cycling performance of Li @Ni foil electrodes when paired with LiFeO₄ cathode in full cell. The cell cycled at current densities of 1 C for a capacity of 1 mAh cm⁻².

Table S1. The cycle life of full cells using 3D hosts based Li-metal composite anodes

Anode	Current density/ mA cm ⁻²	Cycling number	Reference	Cathode, Capacity/ mAh cm ²
Li/Al ₄ Li ₉ -LiF	1.65	150	3	LTO, 3.3
Li-coated PI	1.5	100	4	LTO, 3
Li@porous Cu	0.5	100	5	LFP, 1
Li@NGCFs (nitrogen-doped graphitic carbon foams)	2.2	200	6	LFP, 2.2
ZnO decorated CuNWs membrane	4.25	100	7	LiCoO ₂ , 0.85
Li@Hollow carbon spheres	1	50	8	LFP, 1
Li/VA CuO-Cu	10	5	9	LFP, 2
Li@SirGO (Si nanoparticles embedded reduced graphene oxide)	1.25	375	10	NMC532, 2.5
Li @3D MXene/Graphene framework	0.35	100	11	LTO, 0.35
Li@ nanoporous N-doped graphene	0.09	500	12	LFP, 0.45
3D TiC/C Core/Shell Nanowire	2.55	200	13	LFP, 0.51
Li@3D Porous Cu	0.15	300	14	LFP, 0.3
Li@ CuNW-P (copper nanowire-phosphide)	0.25	300	15	LFP, 0.51
Li@Crumpled Graphene Balls	0.68	500	16	LFP, 1.36
Li/CF@PAN	1	200	17	NCM523, 2.5
Li@ NHCNSs (N-doped hollow carbon nanospheres)	2.72	200	18	LFP, 2.72
Li@MgZnO/CNF-rGO	3	500	19	LFP, 0.6
Li@3D Ni foam	3.18	100	20	LTO, 6.36
Li@3D-AGBN (silver nanowire and graphene-based binary network)	2.25	1000	21	NCM523, 0.22
Li@G-CNF	0.34	300	22	LFP, 0.34
Li@3D N-Ni	3.4	1500	This work	LFP, 0.68

Note: The Li composite anodes for comparison were built via depositing Li on 3D modified frames. To clearly distinguish the contribution of anode structure to the capacity retention, cells with cathode materials owning good cycling stability such as LFP, LTO, LiCoO₃ and NCM, rather than

the ones with sulfur cathodes, were listed. The current densities were calculated by areal capacity multiply rate, which was supposed to make a fair comparison between different literatures. The longer cycle and higher current densities would be chosen if the cycling performance were measured under different conditions.

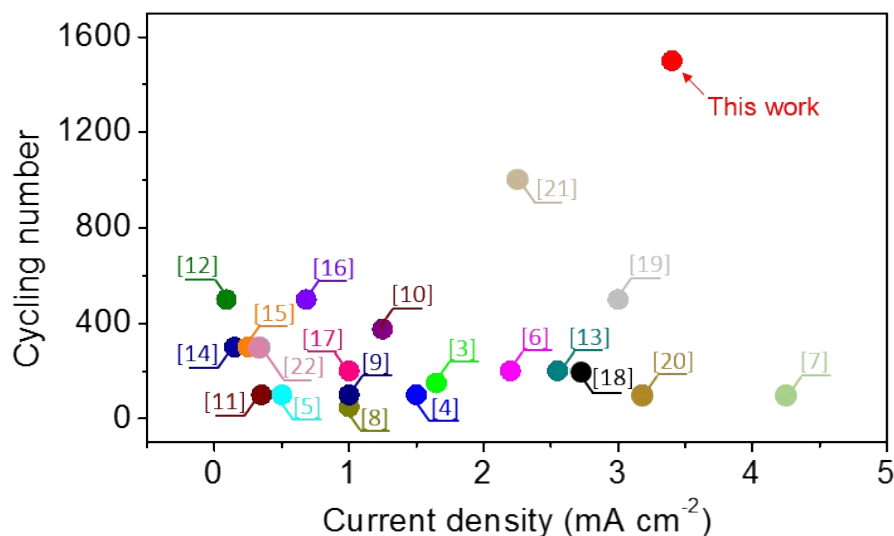


Fig. S11 Comparison of the cycle life of full cells using Li@3D N-Ni anode and various Li-metal composite anodes based on Table S1.

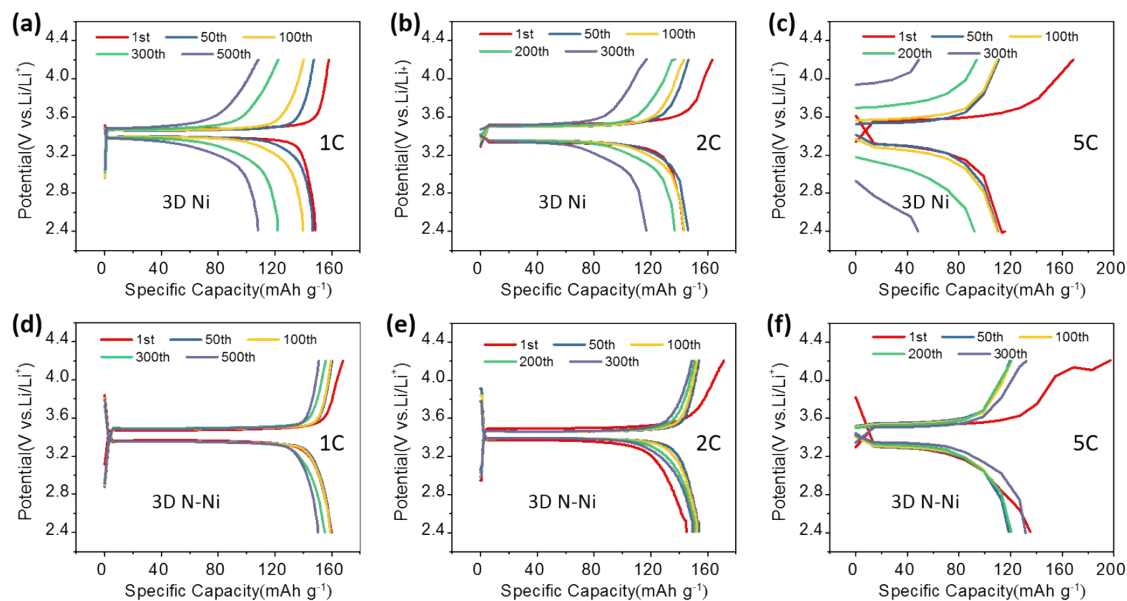


Fig. S12 Galvanostatic discharge/charge curves of Li@3D Ni||LFP (a-c) and Li@3D N-Ni||LFP (d-f) cells at 1 C, 2 C and 5 C (1C= 170 mAh g⁻¹).

References

1. J. Huang, Y. Sun, X. Du, Y. Zhang, C. Wu, C. Yan, Y. Yan, G. Zou, W. Wu, R. Lu, Y. Li and J. Xiong, *Advanced Materials*, 2018, **30**, 1803367.
2. P. Liu, J. Ran, B. Xia, S. Xi, D. Gao and J. Wang, *Nano-Micro Letters*, 2020, **12**, 68.
3. H. Wang, D. Lin, Y. Liu, Y. Li and Y. Cui, *Science Advances*, 2017, **3**, e1701301.
4. Y. Liu, D. Lin, Z. Liang, J. Zhao, K. Yan and Y. Cui, *Nature Communications*, 2016, **7**, 10992.
5. S.-H. Wang, Y.-X. Yin, T.-T. Zuo, W. Dong, J.-Y. Li, J.-L. Shi, C.-H. Zhang, N.-W. Li, C.-J. Li and Y.-G. Guo, *Advanced Materials*, 2017, **29**, 1703729.
6. L. Liu, Y.-X. Yin, J.-Y. Li, S.-H. Wang, Y.-G. Guo and L.-J. Wan, *Advanced Materials*, 2018, **30**, 1706216.
7. L.-L. Lu, J. Ge, J.-N. Yang, S.-M. Chen, H.-B. Yao, F. Zhou and S.-H. Yu, *Nano Letters*, 2016, **16**, 4431-4437.
8. G. Zheng, S. W. Lee, Z. Liang, H.-W. Lee, K. Yan, H. Yao, H. Wang, W. Li, S. Chu and Y. Cui, *Nature Nanotechnology*, 2014, **9**, 618-623.
9. C. Zhang, W. Lv, G. Zhou, Z. Huang, Y. Zhang, R. Lyu, H. Wu, Q. Yun, F. Kang and Q.-H. Yang, *Advanced Energy Materials*, 2018, **8**, 1703404.
10. H. Wang, X. Cao, H. Gu, Y. Liu, Y. Li, Z. Zhang, W. Huang, H. Wang, J. Wang, W. Xu, J.-G. Zhang and Y. Cui, *ACS Nano*, 2020, **14**, 4601-4608.
11. H. Shi, C. J. Zhang, P. Lu, Y. Dong, P. Wen and Z.-S. Wu, *ACS Nano*, 2019, **13**, 14308-14318.
12. G. Huang, J. Han, F. Zhang, Z. Wang, H. Kashani, K. Watanabe and M. Chen, *Advanced Materials*, 2019, **31**, 1805334.
13. S. Liu, X. Xia, Y. Zhong, S. Deng, Z. Yao, L. Zhang, X.-B. Cheng, X. Wang, Q. Zhang and J. Tu, *Advanced Energy Materials*, 2018, **8**, 1702322.
14. Q. Yun, Y.-B. He, W. Lv, Y. Zhao, B. Li, F. Kang and Q.-H. Yang, *Advanced Materials*, 2016, **28**, 6932-6939.
15. C. Zhang, R. Lyu, W. Lv, H. Li, W. Jiang, J. Li, S. Gu, G. Zhou, Z. Huang, Y. Zhang, J. Wu, Q.-H. Yang and F. Kang, *Advanced Materials*, 2019, **31**, 1904991.
16. S. Liu, A. Wang, Q. Li, J. Wu, K. Chiou, J. Huang and J. Luo, *Joule*, 2018, **2**, 184-193.
17. P. Shi, X.-Q. Zhang, X. Shen, B.-Q. Li, R. Zhang, L.-P. Hou and Q. Zhang, *Advanced Functional Materials*, 2021, **31**, 2004189.
18. Y. Liu, Y. Zhen, T. Li, F. Bettels, T. He, M. Peng, Y. Liang, F. Ding and L. Zhang, *Small*, 2020, **16**, 2004770.
19. T. Le, C. Yang, Q. Liang, X. Huang, F. Kang and Y. Yang, *Small*, 2021, **17**, 2007231.
20. S.-S. Chi, Y. Liu, W.-L. Song, L.-Z. Fan and Q. Zhang, *Advanced Functional Materials*, 2017, **27**, 1700348.
21. P. Xue, S. Liu, X. Shi, C. Sun, C. Lai, Y. Zhou, D. Sui, Y. Chen and J. Liang, *Advanced Materials*, 2018, **30**, 1804165.
22. Y. Nan, S. Li, Y. Shi, S. Yang and B. Li, *Small*, 2019, **15**, 1903520.